

## Surface Science Letters

# On the formation of Ar–Kr two-dimensional mixtures

Peter Zeppenfeld <sup>a</sup>, Ulrich Becher <sup>a</sup>, Klaus Kern <sup>b</sup>, Rudolf David <sup>a</sup> and George Comsa <sup>a</sup>

<sup>a</sup> Institut für Grenzflächenforschung und Vakuumphysik, Forschungszentrum Jülich, D-52425 Jülich, Germany

<sup>b</sup> Institut de Physique Expérimentale, EPF Lausanne, PHB-Ecublens, CH-1015 Lausanne, Switzerland

Received 2 August 1993; accepted for publication 31 August 1993

Successive adsorption of submonolayer amounts of Kr and Ar onto a Pt(111) surface leads to the formation of separate 2D islands of almost pure Kr and Ar content. Upon annealing, the phase separated Kr and Ar start to mix resulting eventually in a complete stochastic mixture of the two components at about  $T_{\text{mix}} = 30\text{--}36$  K, depending on the Ar:Kr mixing ratio. This continuous mixing transition proceeds primarily via the dissolution of Kr atoms into the Ar 2D islands and not vice versa, as might be expected for kinetic reasons. Instead, the intermixing behaviour can be explained by the fact that the binding between an Ar and a Kr atom is stronger than between two Ar atoms but weaker than between two Kr atoms. As a consequence the incorporation of a Kr atom from the edge of an Ar island into its center is energetically favored while the dissolution of Ar into Kr is hindered.

The study of bulk alloys is a topic of continuous scientific and technological interest. The mixing of two or more material components can lead to the formation of a homogeneous alloy or several separate phases may coexist. Even simple, two-component (binary) mixtures can exhibit quite complex phase diagrams comprising a wealth of different ordered and disordered structures depending on the mixing ratio, temperature, and pressure. As a consequence, bulk alloys are frequently used as model candidates in the study of thermodynamics [1] and disorder [2] of solids. Besides the characterization of the *equilibrium* state of a mixture also the *kinetic* processes, such as interdiffusion and segregation within the mixture, are of great fundamental interest and practical importance.

Several new phenomena occur at the *surface* of an alloy: The concentration of the individual components, the ordering, and the structure at the surface may be quite different from what would be anticipated from a mere truncation of the bulk alloy. For instance, in the case of a binary alloy a characteristic surface concentration profile of the two components A and B will result from the interplay between the difference in the

surface free energies of the two components and the “interchange energy”  $J$ , defined as  $J = E_{\text{AB}} - \frac{1}{2}(E_{\text{AA}} + E_{\text{BB}})$  where  $E$  denotes the binding energies between like (AA and BB) and unlike (AB) pairs of atoms: The concentration of the component with the lowest surface free energy (say A) will be enhanced in the topmost layer. If, in addition,  $J < 0$  (i.e., if the mixing of the two components is energetically preferred) the system will seek to maximize the number of AB pairs and as a consequence the second layer will be enriched in component B and the third layer again in component A [3]. Thus, a complex, oscillatory concentration profile is obtained. In real samples, the segregation *kinetics* will also have an important impact on the actual composition of the surface. External perturbations such as a change in temperature or the sputtering of the surface will affect the concentration profiles, while the diffusion from the bulk will try to re-establish the equilibrium profile [4].

We have recently proposed a physical realization for alloys in *two dimensions*, namely the binary mixtures of sub-monolayer amounts of rare gas species adsorbed on a single-crystal surface [5]. In analogy with binary bulk alloys in three

dimensions (3D), these systems can serve as model systems in the study of disorder in two dimensions (2D). The disorder which is introduced by mixing the two components originates from the size mismatch of the two types of rare gas atoms. We find that for small size mismatch of  $\leq 10\%$  (i.e., in the case of the Kr–Xe and Ar–Kr systems) the mixtures form periodically ordered phases for all composition ratios [5,6] while in the case of the Ar–Xe mixture, characterized by a large size mismatch of about 17%, only short range ordered “amorphous” structures are obtained. This result is in close analogy to the empirical “Hume-Rothery rule” formulated for the case of bulk alloys [7] and is also in close agreement with experiments [8] and computer simulations [9] of non-interacting discs.

Here, we want to focus on the mixing transition in the case of the Ar–Kr system adsorbed on the Pt(111) surface trying to reveal some details on the thermodynamics and the role played by kinetics in such two-dimensional alloys. To this end we have prepared the phase separated Ar + Kr system at low temperature and studied its evolution towards the complete, homogenous mixture with increasing temperature.

The experimental set-up used in the experiments is described in detail in ref. [10]. In brief, a supersonic He beam is generated by expanding He gas from a pressure of about 150 bar through a small nozzle (5  $\mu\text{m}$  in diameter). The resulting He beam is highly monochromatic ( $\Delta E/E = 1.4\%$ ). It is directed at the sample and the scattered He atoms are detected in a quadrupole mass spectrometer. The total scattering angle is fixed ( $\theta_i + \theta_f = 90^\circ$ ) and the scattering conditions are varied by rotating the sample about an axis normal to the scattering plane yielding a parallel momentum transfer  $Q = k_i(\sin \theta_i - \sin \theta_f) = \sqrt{2}k_i \sin(\theta_i - 45^\circ)$ . The azimuthal orientation of the sample can be varied by rotating the crystal about its surface normal. The angular divergence of the incident beam and the angle subtended by the detector are both  $0.2^\circ$ . Together with the energy spread of the incident beam this results in a wave vector resolution of the apparatus of about  $0.01 \text{ \AA}^{-1}$ . The sample temperature can be varied between 20 and 1500 K. The Pt(111) sam-

ple is a high quality surface with an average terrace width  $\geq 2000 \text{ \AA}$  [11]. It was cleaned by cycles of Ar sputtering and heating in oxygen until no traces of impurities could be detected by Auger spectroscopy. Before each experiment the sample was cleaned by sputtering with Ar and subsequent annealing at about 1000 K. The sample smoothness and cleanliness were routinely checked by monitoring the He reflectivity, which constitutes a sensitive probe for surface defects and impurities [12].

The rare gases were adsorbed onto the Pt(111) substrate by exposing the sample to a partial pressure of the rare gas. The amount adsorbed on the surface (i.e., the coverage) can be accurately determined by monitoring the decrease of the He reflectivity as a function of exposure [13]. Once this coverage calibration is established the desired rare gas coverage can be controlled within an estimated error of  $\pm 5\%$  by dosing the appropriate amount. In the present case the two components Ar and Kr were adsorbed successively. By monitoring the He reflectivity, it was checked that the presence of one component does not modify (within the accuracy of our experiment) the adsorption properties of the other component as compared to the adsorption on the clean Pt(111) surface. Besides the total coverage the most important parameter used for the characterization of the mixture is the relative composition. In the following we will use the molar fraction  $\chi$  defined as the ratio between the number of Ar atoms and the total number of Ar and Kr atoms on the surface to quantify the composition of the mixture. The molar fraction is easily obtained from the measured partial Ar and Kr coverages. In the following, we will only report results obtained from mixtures in the sub-monolayer regime (i.e., where the total Ar plus Kr coverage is below one monolayer).

Once the two components are adsorbed on the surface the structure is investigated by taking polar and azimuthal diffraction scans yielding the size and orientation of the unit cell. If the rare gases are adsorbed at low surface temperature ( $\leq 25 \text{ K}$ ) separate Ar and Kr  $n$ th order diffraction peaks are observed indicating the formation of two distinct hexagonal phases on top of the

underlying Pt(111) substrate. The wave vector positions of the diffraction peaks are close to those found for the pure Ar and Kr phases, indicating that at these low temperatures Ar and Kr are still phase separated. However, the *orientation* of the adsorbate structures critically depends on the adsorption sequence: If Ar is adsorbed on the clean Pt(111) surface a hexagonal Ar phase is obtained whose orientation is *aligned* ( $R0^\circ$ ) with respect to the substrate (i.e., in which the high symmetry directions of the adsorbate structure are collinear with those of the substrate surface). Adsorption of Kr on the so prepared surface yields Kr 2D islands which are also oriented in an aligned phase. On the other hand, if first Kr is adsorbed on the clean Pt(111) surface a *rotated*  $R30^\circ$  Kr phase is obtained and subsequent adsorption of Ar results in the formation of Ar 2D islands which then also exhibit the rotated  $R30^\circ$  orientation. Hence, the presence of the first rare gas species has a decisive impact on the nucleation of the second. The same effect on the orientation of the Kr and Ar adlayer has already been observed previously for various pre-adsorbed impurities (such as H, CO, or Xe) [14,15]. It has been ascribed to the different growth of the 2D rare gas islands at steps and on the Pt(111) terraces, respectively [14]: On the clean surface the nucleation of the 2D islands proceeds at the step edges (which are always present even on a “smooth” substrate); if these step edges are blocked by adsorption of H, CO or another rare gas, the islands apparently nucleate on the free (111) terraces and grow with a different orientation ( $R30^\circ$  instead of  $R0^\circ$  in the case of Ar and  $R0^\circ$  instead of  $R30^\circ$  in the case of Kr).

An additional phenomenon which is observed upon depositing the second rare gas is the compression of the previously adsorbed Ar or Kr phase (see also figs. 1a and 1b). This again is not unexpected, since it was shown previously that with increasing coverage already the *pure* Ar and Kr phases adsorbed on Pt(111) undergo phase transitions in which the structures are compressed to form high-order commensurate phases [16,17]. Only, in the present case, the compression is accomplished using the spreading pressure of a different rare gas species. In fig. 1, for

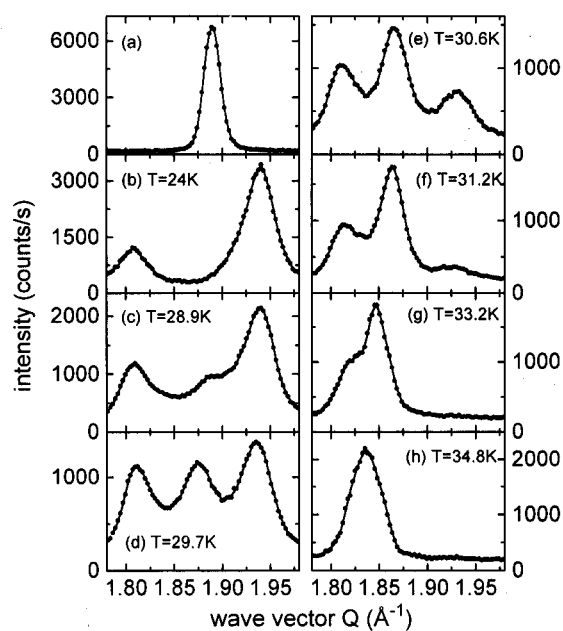


Fig. 1. He-diffraction scans across the first order diffraction peaks for an Ar–Kr binary mixture adsorbed on a Pt(111) substrate. (a) After adsorption of 0.27 monolayers of Ar ( $2.11 \times 10^{14}$  atoms per  $\text{cm}^2$ ) at 24 K. (b) After further adsorption of  $1.44 \times 10^{14} \text{ cm}^{-2}$  of Kr yielding a total coverage of  $3.55 \times 10^{14} \text{ cm}^{-2}$  and an Ar molar fraction of  $\chi_{\text{Ar}} = 0.59$ . (c)–(h): changes in the diffraction signature upon increasing the surface temperature to 28.9 K (c), 29.7 K (d), 30.6 K (e), 31.2 K (f), 33.2 K (g) and 34.8 K (h).

instance, a quarter of a monolayer of Ar was adsorbed prior to about the same amount of Kr at 24 K. In this case separate 2D Ar and Kr phases in the aligned  $R0^\circ$  orientation are formed. From the wave vector position  $Q_{\text{Ar}} = 1.89 \text{ \AA}^{-1}$  of the first order Ar diffraction peak (fig. 1a) an Ar nearest neighbor distance  $a_{\text{Ar}} = 4\pi/(\sqrt{3} Q_{\text{Ar}}) = 3.84 \text{ \AA}$  is obtained, characteristic for the unconstrained Ar phase [17]. After Kr adsorption the Ar diffraction peak is shifted to  $Q_{\text{Ar}} = 1.94 \text{ \AA}^{-1}$ , corresponding to a slightly compressed phase in which  $a_{\text{Ar}} = 3.74 \text{ \AA}$ . While the latter phase is not yet the dense ( $4 \times 4$ ) phase ( $a_{\text{Ar}} = 3.69 \text{ \AA}$ ) found near monolayer completion in the pure Ar system [17] the compression takes place already at a relatively low Ar + Kr coverage of about half a monolayer. Furthermore, the Kr diffraction peak at  $Q_{\text{Kr}} = 1.81 \text{ \AA}^{-1}$  ( $a_{\text{Kr}} = 4.01 \text{ \AA}$ ) indicates that also the Kr phase is compressed as compared to

the pure, unconstrained Kr phase (characterized by a nearest neighbor distance of 4.10 Å).

If the phase separated Ar–Kr system is prepared as described above, increasing the surface temperature results in the formation of a partially mixed Ar–Kr phase until eventually a complete homogenous mixture is obtained. This is illustrated in figs. 1c–1h which show polar diffraction scans of the first order diffraction features as a function of surface temperature: Upon annealing a third diffraction peak emerges which is located between those of the initial Ar and Kr phases. With increasing temperature this peak gains in intensity and shifts to lower  $Q$  values towards the Kr diffraction peak. The Kr and Ar diffraction peaks remain at their original position although the Ar peak intensity strongly decreases with temperature. Between 31 and 35 K the strong Kr diffraction signature suddenly disappears and only the single diffraction peak at the intermediate position remains. This indicates the formation of a complete stochastic mixture of Ar and Kr atoms, while the crystallographic arrangement of the atoms is still well ordered. Indeed, it was already shown for the case of Kr and Xe adsorbed on the Pt(111) surface [5] that such a structurally ordered, compositionally stochastic mixture is characterized by a single intermediate diffraction peak stemming from an “average lattice” in which the nearest neighbor distance is determined by the composition ratio, ranging between the values of the pure components. At lower surface temperature the presence of residual Kr and Ar diffraction peaks indicates that Ar and Kr do only partially mix and the continuous shift of the intermediate diffraction peak towards the Kr peak position can be interpreted as a continuous enrichment of the Kr component in the mixed phase. This becomes even more evident from fig. 2 where we plot the nearest neighbor distances (surface lattice parameter) as obtained from the position of the diffraction peaks as a function of surface temperature. Clearly, the increase of the Kr content in the mixed phase as well as the almost unaffected position of the Kr diffraction peak up to 33 K can only be explained by the fact that with increasing temperature more and more Kr is incorporated into the Ar rich phase and not vice

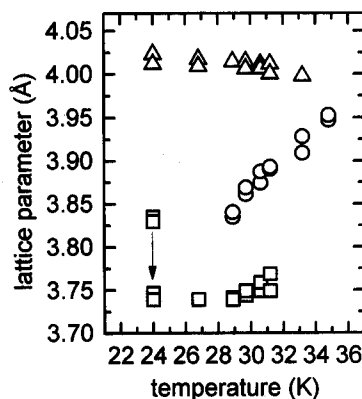


Fig. 2. Average nearest neighbor distance (surface lattice parameter) with increasing surface temperature obtained from the position of the diffraction peaks from the Ar–Kr mixture in fig. 1. The arrow indicates the initial compression of the Ar phase after Kr adsorption.  $\square$ : Ar phase,  $\Delta$ : Kr phase,  $\circ$ : mixed phase.

versa. Therefore, the mixing occurs primarily via the diffusion of Kr into the Ar 2D phase while the diffusion of Ar into Kr appears to be hindered. This observation cannot be explained in terms of surface diffusion and the fact that the Ar atoms would not reach the 2D Kr islands, because the Ar atoms can be expected to have a *higher* surface mobility than the Kr atoms. Hence the exactly *opposite* behavior (namely the enhanced diffusion of Ar into Kr) would be anticipated on the basis of kinetics alone.

In order to explain the intermixing behavior it is necessary to consider the mixing energetics: As already mentioned in the introduction, in the case of bulk alloys, the surface will be enriched in the component of the species with the lowest surface free energy. Similarly, in a two-dimensional system, the edge of a 2D island will be enriched with the component of lowest edge free energy. As a consequence a net concentration gradient of this component will be established through “edge segregation”. In the microscopic picture the edge energy is directly related to the lower binding energy of an edge atom as compared to an atom inside the 2D islands due to the reduced number of nearest neighbors. In the present case the following relation holds for the

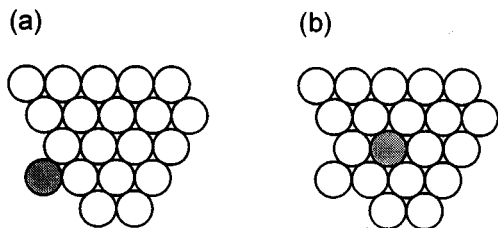


Fig. 3. Schematic illustration of the adsorption of (a) an atom of kind A (hatched circle) at the edge of a 2D island consisting of atoms of kind B (open circles) and (b) the exchange of the A atom and an atom of type B from the center of the island. Depending on the difference of the binding energies  $E_{AB}$  and  $E_{BB}$  between atoms A and B and between two B atoms, respectively, the interdiffusion of atom A into the B island is energetically favored ( $E_{AB} - E_{BB} < 0$ ) or hindered ( $E_{AB} - E_{BB} > 0$ ).

binding energies for the different combinations of pairs of Ar and Kr atoms [18]:

$$E_{KrKr} < E_{ArKr} < E_{ArAr}. \quad (1)$$

(Note that the binding energies are treated as negative numbers). At the edge of a 2D Ar island an arriving Kr atom can only bind to 2 Ar atoms if it adsorbs on a flat edge (or 3 Ar atoms if it occupies a kink site). However, if it exchanges position with an Ar atom in the second row, its nearest neighbor (Ar–Kr) coordination number will be six while the formerly sixfold coordinated Ar atom now occupies the edge or kink site (see also fig. 3). The net energy difference (disregarding the extra contribution to the entropy) will then be 4 (or 3) times the difference between the Ar–Kr and Ar–Ar binding energy ( $E_{ArKr} - E_{ArAr}$ ). Since this difference is *negative*, the dissolution of a Kr atom into a 2D Ar island is energetically favored. On the other hand, if an Ar atom arrives at the edge of a 2D Kr island the exchange with a Kr atom in the center of the 2D island would involve a *positive* energy of a multiple of ( $E_{ArKr} - E_{KrKr}$ ) and thus the dissolution of Ar into Kr is energetically hindered. This exactly reflects the experimental observation. We therefore believe that the energetically favored interdiffusion of Kr into 2D islands of Ar together with the activation barrier for the diffusion of Ar into 2D Kr islands is the origin of the observed mixing behavior.

The transition from the phase separated system to the complete stochastic mixture as depicted in fig. 1 is irreversible: Once the Ar and Kr are partially or completely mixed, cooling the system to the lowest achievable temperature of about 20 K does not lead to a de-mixing of the two components. Whether a mixed or phase separated system is expected depends on the value of the interchange energy  $J$ . Unfortunately, exact values for  $J = E_{ArKr} - \frac{1}{2}(E_{ArAr} + E_{KrKr})$  for Ar and Kr adsorbed on the Pt(111) surface are not available. An approximate value for  $J$  can, however, be extracted from the calculated Ar–Kr mixing energy on Ag(111) [18] yielding  $J \approx 6$  K. (Using the bare gas-phase Lennard-Jones potentials  $J = 10$  K is obtained [18].)  $J > 0$  would indicate that at zero temperature the phase separated system is energetically preferred. With increasing surface temperature the mixing entropy reduces the free energy of the mixed system with respect to the phase separated system leading to a partial and eventually a complete mixing of the two components at higher temperatures. For a stochastic compositional mixture a single homogeneously mixed phase is expected at temperatures above  $T_{\text{mix}} \leq 3J$  [1], where the equal sign stands for the  $\chi_{Ar} = \chi_{Kr} = 0.5$  mixture. At these low temperatures ( $T \leq 20$  K) the surface mobility at least for Kr is rather low. This suggests that the de-mixing is kinetically hindered. The mixing temperatures actually observed in the experiment (e.g.  $T_{\text{mix}} \approx 34$  K in fig. 2) ranges between 31 and 36 K depending on the Ar:Kr mixing ratio. It is largest for the heavily mixed systems ( $\chi_{Ar} = \chi_{Kr} = 0.5$ ) and lower for the dilute mixtures. For all composition ratios we observe a finite miscibility of Kr into Ar which increases with temperature in a similar fashion as illustrated in figs. 1 and 2 for  $\chi_{Ar} = 0.59$ . If the Ar–Kr system at intermediate temperature is only partially mixed a complete mixture can usually be obtained by adding more of the majority component, thereby diluting the mixture. This works particularly well in the case where Ar is added to mixtures with  $\chi_{Ar} > 0.5$ .

While figs. 1 and 2 illustrate the mixing transition in the case where Ar is adsorbed prior to Kr (i.e., where the separate Ar and Kr phases as well as the mixed phase are in the aligned  $R0^\circ$  orien-

tation) a similar situation arises if Kr is adsorbed prior to Ar: At low temperature separate Kr and Ar phases are observed, but both with the rotated R30° orientation. Increasing the temperature again leads to an increasing miscibility of Kr in Ar while the Ar dissolution in Kr only sets in at higher temperature. The partial mixture as well as the complete stochastic mixture just above the mixing temperature are also oriented in the rotated R30° phase. This result seems to be in contradiction with the aligned R0° orientation observed for the complete mixture if Ar is adsorbed prior to Kr. However, annealing the aligned R0° mixed phase at higher temperatures ( $\approx 40$  K) usually leads to a partial population of the rotated R30° phase. Therefore, the R30° orientation of the mixture appears to be energetically preferred, but the transition from the metastable R0° to the R30° phase is obviously kinetically hindered. Unfortunately, the transition from the R0° to the R30° mixed phase cannot be studied until the rotation is complete since above 40 K the Ar desorption becomes significant and the mixture is continuously enriched in Kr (which as a pure phase on the Pt(111) surface also nucleates in a R30° oriented phase).

We want to close our discussion on the mixing transition of the 2D Ar–Kr system by mentioning that the compositionally mixed systems (in both the R0° and the R30° orientation) form crystallographically well ordered, periodic structures for all composition ratios. In this respect we find a very similar behavior as observed previously for the Kr–Xe system on Pt(111) [5]. In fact, one of the most important parameters determining the structural order of a mixture is the relative size of the atomic diameters of the two components. This parameter is similar for the Ar–Kr and the Kr–Xe system (0.94 and 0.91, respectively). As for the Kr–Xe complete mixture, the two components Ar and Kr are randomly distributed and the diffraction signature from the mixed phase can be viewed as stemming from an *average lattice* whose properties (lattice constant and positional order) are determined by the Ar:Kr mixing ratio. In fig. 4 we have plotted the “average” nearest neighbor distance in the completely mixed Ar–Kr phase as obtained from the position of the

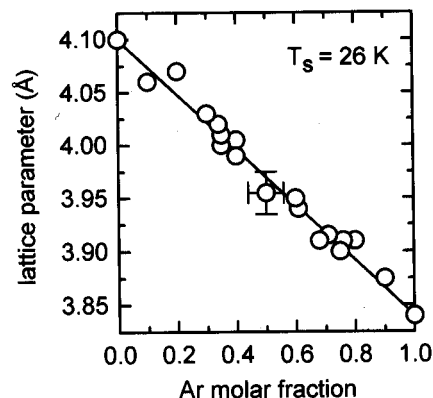


Fig. 4. Surface lattice parameter of the complete Ar–Kr mixture as obtained from the He-diffraction peak position as a function of the Ar molar fraction  $\chi_{Ar}$ . The mixtures were prepared by adsorbing Ar after Kr. After annealing, the resulting mixed phase is in the rotated R30° orientation. The measurements were all carried out at about 26 K. The solid line corresponds to the linear interpolation between the lattice parameter of the pure, unconstrained Ar and Kr phases (Vegard's law).

diffraction peak (in this case for the R30° oriented phase). This “average” lattice parameter varies with the molar fraction in a continuous, linear fashion between the nearest neighbour distances of the pure, unconstrained Ar and Kr components ( $a_{Ar} = 3.84$  Å and  $a_{Kr} = 4.10$  Å, respectively):

$$a = \chi_{Ar} a_{Ar} + (1 - \chi_{Ar}) a_{Kr}. \quad (2)$$

The same relationship, known as “Vegard's law” [19], is also observed for the aligned R0° Ar–Kr mixed phase [20] as well as for the Kr–Xe mixtures on Pt(111) [5].

The authors gratefully acknowledge stimulating discussions with R.B. Gerber and A.T. Yinnon.

## References

- [1] R.A. Swalin, *Thermodynamics of Solids* (Wiley, New York, 1972) chs. 9 and 11.
- [2] J.M. Ziman, *Models of Disorder* (Cambridge University Press, Cambridge, 1979).
- [3] V.S. Sundaram and P. Wynblatt, *Surf. Sci.* 52 (1975) 569.
- [4] J. Kirschner, *Nucl. Instrum. Methods B* 7/8 (1985) 742.

- [5] P. Zeppenfeld, U. Becher, K. Kern, R. David and G. Comsa, *Surf. Sci. Lett.* 285 (1993) L461; M. Yanuka, A.T. Yinnon, R.B. Gerber, P. Zeppenfeld, K. Kern, U. Becher and G. Comsa, *J. Chem. Phys.*, submitted.
- [6] R.B. Gerber and A.T. Yinnon, *Chem. Phys. Lett.* 181 (1991) 553; R.B. Gerber, A.T. Yinnon, M. Yanuka and D. Chase, *Surf. Sci.* 272 (1992) 81.
- [7] W. Hume-Rothery, R.E. Smallman and C.W. Harworth, *The Structure of Metals and Alloys* (The Metals and Metallurgy Trust, London, 1969); J.L. Barrat, M. Baus and J.P. Hansen, *Phys. Rev. Lett.* 56 (1986) 1063.
- [8] A.S. Nowick and S.R. Mader, *IBM J. Res. Dev.* Sept./Nov. (1965) 348.
- [9] D.R. Nelson, M. Rubinstein and F. Saepen, *Philos. Mag.* A 46 (1982) 105; M. Rubinstein and D.R. Nelson, *Phys. Rev. B* 26 (1982) 6254.
- [10] R. David, K. Kern, P. Zeppenfeld and G. Comsa, *Rev. Sci. Instrum.* 57 (1986) 2771.
- [11] B. Poelsema, R.L. Palmer, G. Mechtersheimer and G. Comsa, *Surf. Sci.* 117 (1982) 60.
- [12] B. Poelsema and G. Comsa, *Scattering of Thermal Energy Atoms from Disordered Surfaces*, Springer Tracts in Modern Physics, Vol. 115 (Springer, Berlin, 1989).
- [13] K. Kern and G. Comsa, in: *Kinetics of Ordering and Growth at Surfaces*, Ed. M. G. Lagally (Plenum, New York, 1990) 53.
- [14] K. Kern, P. Zeppenfeld, R. David, R.L. Palmer and G. Comsa, *Phys. Rev. Lett.* 57 (1986) 3187.
- [15] K. Kern, P. Zeppenfeld, R. David and G. Comsa, *J. Vac. Sci. Technol. A* 6 (1988) 639.
- [16] K. Kern, P. Zeppenfeld, R. David and G. Comsa, *Phys. Rev. Lett.* 59 (1987) 79.
- [17] P. Zeppenfeld, U. Becher, K. Kern and G. Comsa, *Phys. Rev. B* 45 (1992) 5179.
- [18] N.K. Mahale and M.W. Cole, *Surf. Sci.* 176 (1986) 319.
- [19] L. Vegard and Hjalmar Dale, *Z. Kristallogr.* 67 (1928) 148.
- [20] For instance, the position of the diffraction peak from the mixed  $R0^\circ$  Ar-Kr phase in fig. 1h at  $Q = 1.835 \text{ \AA}^{-1}$  corresponds to an average nearest neighbor distance of  $3.95 \text{ \AA}$ . The value obtained from eq. (2) using  $a_{\text{Ar}} = 3.84$ ,  $a_{\text{Kr}} = 4.10$ , and  $\chi_{\text{Ar}} = 0.59$  is  $a = 3.947 \text{ \AA}$ , in excellent agreement with the experimental value.